European Review for Medical and Pharmacological Sciences 2019; 23 (3 Suppl): 294-303

Aldose reductase inhibitor Epalrestat alleviates high glucose-induced cardiomyocyte apoptosis *via* ROS

X. WANG[1], F. YU[2], W.-Q. ZHENG[3]

[1]Department of Pharmacy, Weihai Central Hospital, Weihai, China
[2]Department of Dermatology, Weihai Central Hospital, Weihai, China
[3]Department of Cardiology, Weihai Central Hospital, Weihai, China

Abstract. – OBJECTIVE: To clarify the role of aldose reductase inhibitor (ARI) in the high glucose-induced cardiomyocyte apoptosis and its mechanism.

MATERIALS AND METHODS: In this study, H9c2 cardiomyocytes were employed as objects, high-glucose medium as stimulus, and ARI Epalrestat as a therapeutic drug. The cell apoptosis and activity changes of nitric oxide synthase (NOS), NO, and reactive oxygen species (ROS) were evaluated *via* Hoechst staining, enzyme-linked immunosorbent assay (ELISA), polymerase chain reaction (PCR), and Western blotting. In addition, the mitochondrial membrane potential was measured *via* fluorescence counting.

RESULTS: Epalrestat inhibited the activity of AR to improve high glucose-induced oxidative stress in cardiomyocytes, weaken ROS activity, relieve the inhibition on NO activity, alleviate mitochondrial membrane potential damage, reduce the level of high glucose-induced cardiomyocyte apoptosis, and suppress the expression and activity of Caspase-3, thereby preventing high glucose-induced cardiomyocyte apoptosis.

CONCLUSIONS: ARI protects against high glucose-induced cardiomyocyte apoptosis.

Key Words:
Aldose reductase inhibitor, High blood glucose, Apoptosis, ROS.

Introduction

With the aging of the population, as well as changes in people's lifestyle, the incidence rate of diabetes is increasing year by year in China, which has become a major public health issue. A survey revealed that over 70% of diabetic patients die of cardiovascular diseases and that the mortality rate is 2-4 times that in non-diabetic population[1]. Therefore, diabetes-related cardiovascular complications are a leading cause of death in diabetic patients. Currently, scholars in China and elsewhere have considered diabetes as an independent risk factor for cardiovascular diseases[2]. High-glucose toxicity is the main factor damaging the heart and vessels, and the degree of such damage is closely correlated with the duration of hyperglycemia and level of blood glucose

Reports[3-5] have manifested that long-term high-glucose cannot only activate the renin-angiotensin-aldosterone system (RAAS), produce reactive oxygen species (ROS), and increase the advanced glycation end products (AGEs), as well as their receptors (RAGEs), but also activate inflammatory response and endoplasmic reticulum stress response, thereby promoting the damage and death of cardiomyocytes and vascular endothelial cells through various pathways. Hence, the current research hotspot is to explore the new mechanism of high glucose-induced damage to cardiomyocytes and vessels, and provide novel targets and measures for the prevention and treatment of diabetes-related cardiovascular complications.

The pathogenesis of diabetes is that glucose fails to be normally transformed into glycogen stores for a long time in the body of patients, thereby triggering the abnormally active reduction pathway of aldose. As a key enzyme in the polyol metabolism pathway, aldose reductase (AR) can reduce glucose into sorbitol which, with strong polarity, does not easily pass through cell membranes, but rather it accumulates in cells to alter the permeability of cells and weaken the

Corresponding Author: Wenqing Zheng, MM; e-mail: zhengwenqing369@163.com

Na^+-K^+-ATPase activity. This resulting in inositol loss and cell metabolism, as well as function impairment[6]. Since the drugs that block or attenuate AR activity can be used to prevent or delay the occurrence of diabetic complications, AR inhibitors (ARIs) have become therapeutic factors in the treatment of diabetes[7].

Thus, it was wondered whether high glucose-induced myocardial injury mechanism in diabetes involves aberrantly active aldose reduction pathways and whether ARIs are capable of improving high glucose-induced myocardial injury. Based on this hypothesis, this work aims to investigate the influence of ARIs on cardiomyocyte apoptosis and the regulatory mechanism of ROS therein, by establishing the high glucose-induced cardiomyocyte apoptosis model using ARIs and detecting AR activity, cell survival rate, ROS level, and changes in apoptosis-related indicators.

Materials and Methods

Culture of Cardiomyocytes

H9c2 cells were purchased from the Shanghai Institute of Biochemistry and Cell Biology, at the Chinese Academy of Sciences (Shanghai, China). The cell suspension was transferred into a 10 mL centrifuge tube and added with 5 mL of Dulbecco's Modified Eagle Medium (DMEM; Gibco, Rockville, MD, USA) containing 10% fetal bovine serum (FBS; Gibco, Rockville, MD, USA). After centrifugation at 1,000 rpm for 10 min, with the supernatant discarded, the cells were added with an appropriate volume of DMEM containing 10% FBS, pipetted and mixed evenly, and their concentration was adjusted to 1×10^5 cells/mL. Next, the cells were inoculated into a 25 mL culture flask and cultured in an incubator with 5% CO_2 at 37°C, and 24 h later, the medium was replaced.

Cell Counting Kit (CCK)-8 Assay

The cells in the logarithmic growth phase were digested, harvested, and prepared into the suspension at the concentration of 1×10^5cells/mL. Subsequently, they were seeded into a 96-well plate (100 μL/well). In the experiment, triplicate wells and blank controls were set. After inoculation overnight, the cells were observed under a microscope to verify whether they adhered well. After treatment, each well of cells was cultured with 20 μL of MTT (3-(4,5-dimethylthiazol-2-yl)-2,5-diphenyl tetrazolium bromide; Sigma-Aldrich, St. Louis, MO, USA) at 37°C for 4 h. Next, with the supernatant sucked away carefully, each well of cells was added with 150 μL of dimethyl sulfoxide (DMSO; Sigma-Aldrich, St. Louis, MO, USA), shaken, and mixed evenly. Finally, the optical density (OD) of each well was measured at the wavelength of 570 nm using a microplate reader. The experiment was repeated for three times.

Determination of Lactate Dehydrogenase (LDH) Content

The cells in the logarithmic growth phase were digested, harvested, and prepared into the suspension at the concentration of 1×10^5cells/mL. Then, they were seeded into a 96-well plate (100 μL/well). In the experiment, triplicate wells and a control group was set. After cell attachment, the culture plates were placed in the incubator at 37°C with 5% CO_2 and cultured for 24 h. A total of 20 μL of the supernatant was obtained from each well, grouped, added with the corresponding reagents according to the kit instructions, mixed evenly, and let stand at room temperature for 3 min. Subsequently, a 1 cm light path cuvette was zeroed at the wavelength of 440 nm using double distilled water, and the OD was determined by means of the microplate reader. The unit is defined as follows: 1,000 mL of culture solution reacts with matrices at 37°C for 15 min and 1 g/mol pyruvic acid produced in the reaction system is regarded as 1 unit. Finally, the content of LDH in the medium was calculated using the formula.

Hoechst Staining

All groups of cells cultured were inoculated into coverslips and treated in different groups, and once the supernatant was removed, they were washed using phosphate-buffered saline (PBS), fixed in Carnoy's solution and rinsed using PBS for 5 min. Then, the cells were stained with Hoechst 33258 working solution, let stand at room temperature for 15 min, rinsed with PBS again and sealed in the mixture of glycerin and PBS (1:1) or water-soluble mounting medium. Finally, the cells were observed under a fluorescence microscope. It was found that the cell nuclei displayed the blue fluorescence spots because the Hoechst stains are the specific fluorescence probe of deoxyribonucleic acid (DNA).

Polymerase Chain Reaction (PCR)

The cells treated were collected from each group to extract total ribonucleic acids (RNAs) using TRIzol (Invitrogen, Carlsbad, CA, USA).

After the concentration of samples was measured, RNAs were reversely transcribed into cDNAs in the first 40 cycles using the reverse transcription system according to the concentration. Then, PCR amplification was performed with the reverse transcription reaction conditions set. After each cycle, the fluorescence signals were collected in a real-time way, while the amplification and dissolution curves were plotted. Primer sequences used in this study were as follows: caspase 3, F: 5'-GTCCGGTACTCTCACTATACAC-3', R: 5'-CGGTAAGGTTGTGTCACTTGGA-3'; NOS, F: 5'-GCCTGACACGGATACTACGGCAG-3', R: 5'-GGATTACAGTCATGGCGCCAAG-3'; GAPDH: F: 5'- CGCTCTCTGCTCCTCCTGTTC -3', R: 5'-ATCCGTTGACTCCGACCTTCAC-3'.

Detection of Caspase-3 Activity

After all groups of cells were collected, washed in PBS, and lysed with trypsin *via* an ice bath, the cell lysates were extracted to absorb cell medium for later use. Then, the adherent cells were digested using trypsin, transferred into the cell culture solution stored, mixed evenly with 2 mM Ac-DE-VD-pNA, and incubated at 37°C for 60-120 min. The absorbance (A value) was measured once the relatively obvious color changes were found.

Western Blotting (WB)

The cells were taken from each group and washed using D-Hank's for 2 times. Then, with the D-Hank's blotted up using absorbent paper, each group of cells was added with 150 μL of pre-cooled lysis buffer and lysed on ice for 30 min. Subsequently, all groups of proteins were collected using a cell scraper, placed in Eppendorf (EP) tubes, and centrifuged at 4°C and 12,000 rpm. The supernatant was sucked and transferred into new EP tubes. After the protein concentration was determined by the bicinchoninic acid (BCA) method (Pierce, Rockford, IL, USA), the proteins were mixed evenly with 5× loading buffer and heated at 100°C for 6 min. A total of 30 μL of proteins were loaded into the wells with prepared separation and spacer gels, while electrophoresis was performed under a proper voltage in the buffer. After that, with the gel clinging to polyvinylidene difluoride (PVDF) membranes (Roche, Basel, Switzerland), the proteins were transferred onto the membranes in the transferring solution at 0°C and a constant voltage of 100 V for 60 min. After that, the PVDF membranes were sealed in 5% skim milk powder at room temperature for 1 h, while the protein bands were cut according to molecular weight and incubated with primary antibodies in a refrigerator at 4°C overnight. On the second day, the PVDF membranes were taken out, rinsed using Tris-Buffered Saline and Tween-20 (TBST), and incubated with the secondary antibody IgG (1:5,000) at room temperature for 1 h. After incubation, the products were rinsed again using TBST, followed by development and measurement of grayscale using Tannon 5200 fluorescent immuno-development system.

Measurement of Inhibition Rate of AR

After being lysed in an ice bath, cells in each group were centrifuged at 4°C. The colorless and transparent supernatant was absorbed. Then, the supernatant was added into a 96-well plate for a reaction which was initiated with the addition of reductive coenzyme II (0.16 mmol/L) and DL-glyceraldehyde substrate (10 mmol/L), while the A value at 340 nm was read continuously using the microplate reader within 40 min. The ability of the inhibitory coenzyme metabolism after the action of the enzyme and substrate represented the activity of AR. Finally, the inhibition curve was plotted with the sample concentration as X-axis and inhibition rate as Y-axis.

Determination of ROS Concentration

The cells at the culture concentration of $6\text{-}8\times10^4$ cells/mL were taken from each group, sub-cultured in the medium for 24 h, and stimulated with stimuli at different concentrations for 8 h. After the culture solution was discarded, the cells were added with the intracellular total ROS probe CM-H2DCFDA at the final concentration of 5 pmol/L and incubated at 37°C in the dark for 30 min. After that, the probe was cleaned using PBS, the products were observed under a confocal laser scanning microscope at the excitation wavelength of 488 nm and an emission wavelength of 515 nm, and green fluorescence was seen. The screenshots of 8-10 cells were acquired in the field of view under a high-power microscope (600×). Finally, the fluorescence intensity was analyzed *via* software.

Determination of Nitric Oxide (NO) Concentration

The NO concentration was determined using the NO detection kit (Applygen Technologies, Beijing, China). After drug pretreatment or uric acid stimulation, the Roswell Park Memorial In-

stitute-1640 (RPMI-1640) medium was replaced with DMEM, and the supernatant of the cell medium was taken, centrifuged, and used for measurement of NO content. All the operations were performed strictly according to the methods in the kit instructions.

Detection of Mitochondrial Membrane Potential

The cells treated were collected and re-suspended in 0.5 mL of cell medium containing serum. Then, they were added with 0.5 mL of JC-1 staining working solution, bottomed up for several times, mixed evenly, and incubated in the incubator at 37°C in the dark for 30 min. The resulting cells were centrifuged at 600 g/min and 4°C, and once the supernatant was discarded, they were washed using 1× JC-1 staining buffer for 2 times, re-suspended in 1× JC-1 staining buffer, and centrifuged as above-mentioned for deposition. The supernatant was removed and the above washing step was repeated once. Finally, the fluorescence intensity was measured using a flow cytometer.

Statistical Analysis

Data were expressed as mean ± SD (standard deviation) and the percentage of those in control group, and analyzed using Statistical Product and Service Solutions (SPSS) 13.0 software (SPSS Inc., Chicago, IL, USA). The comparisons between the two groups were made using independent samples *t*-test. Comparison among multiple groups was made using One-way ANOVA followed by Post-Hoc Test (Least Significant Difference). $p<0.05$ suggested that the data difference was statistically significant.

Results

Action Time Curve in High Glucose-Induced Cardiomyocyte Injury

The cardiomyocytes were treated in the DMEM medium containing 5.5, 22, 33, and 44 mmol/L glucose for 24, 48, and 72 h, respectively. The CCK-8 assay results showed that in the survival rate of cardiomyocytes was lowered in a concentration- and time-dependent manner (Figure 1A), and LDH assay results revealed that the same held true for the degree of cardiomyocyte damage, showing statistically significant differences (Figure 1B, $p<0.05$). Moreover, after treatment with 33 mmol/L glucose for 48 h, the survival rate of cardiomyocytes reached (68.4±5.1)%, so 33 mmol/L and 48 h were taken as the experimental conditions.

Protective Concentration of Epalrestat for Cardiomyocytes Cultured in High Glucose

After being treated using Epalrestat at the concentrations of 1, 10 and 50 μmol/L for 48 h, the survival rate and injury degree of the cardiomyocytes were detected *via* CCK-8 and LDH assays, respectively. It was found that Epalrestat caused significant damage to cardiomyocytes at 50 μmol/L, and the difference was statistically significant (Figure 2, $p<0.05$). Subsequently, the experiment was conducted under the following conditions: Epalrestat at 1 and 10 μmol/L for 48 h.

Epalrestat Protected Cardiomyocytes from High Glucose-Induced Damage

According to the CCK-8 assay results, there was no statistical difference in the survival rate

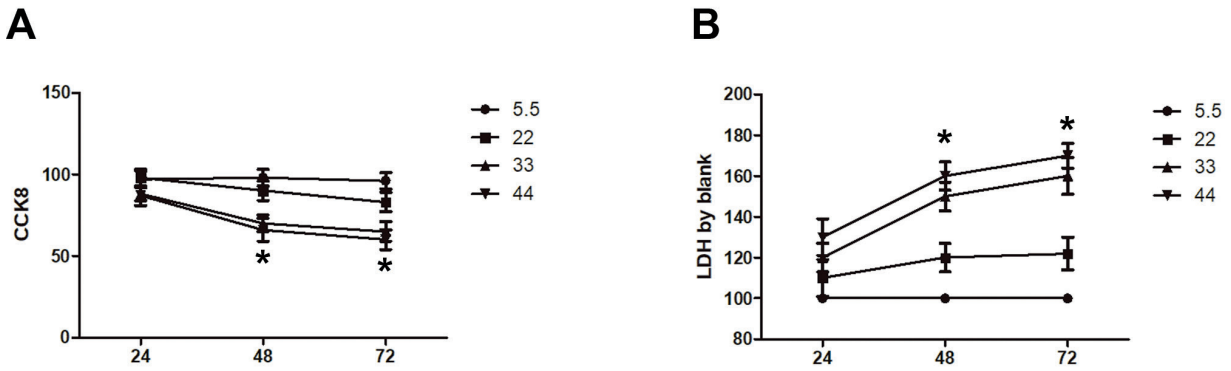

Figure 1. Effects of Glucose on Myocardial Cell Activity. ***A,*** CCK8 detects cell viability after 24h, 48h, and 72h of 5.5, 22, 33, 44 mmol/L glucose treatment. ***B,*** LDH detects cytotoxicity after 24h, 48h, and 72h of 5.5, 22, 33, 44 mmol/L glucose treatment. *compared with 5.5mmol/L glucose, $p< 0.05$.

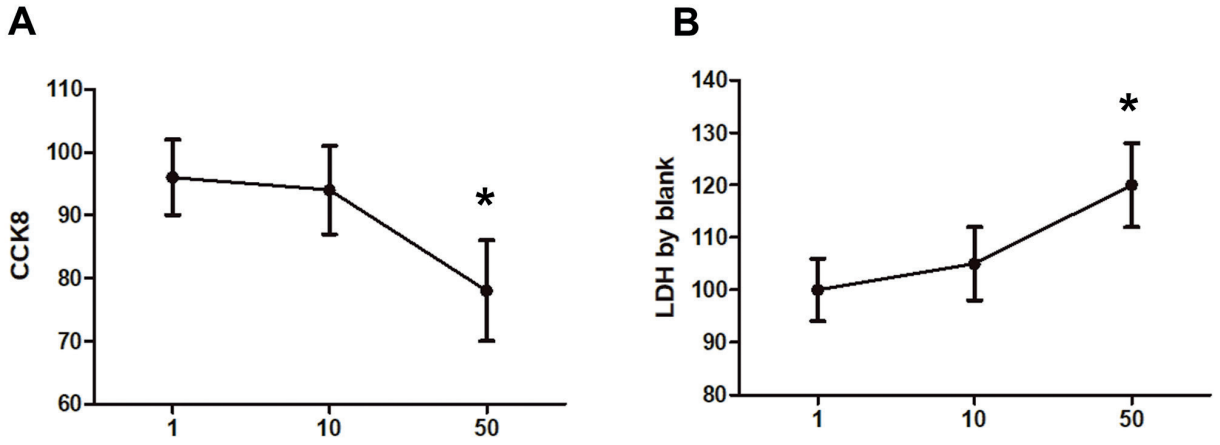

Figure 2. Effect of epalrestat on myocardial cell activity. ***A,*** CCK8 detects cell viability after 48 h after 1, 10, 50 umol/L epalrestat treatment. ***B,*** LDH detects cytotoxicity after 48 h after 1, 10, 50 umol/L epalrestat treatment. * compared with 1 umol/L epalrestat, $p<0.05$.

of cardiomyocytes between normal control group and mannitol group (Figure 3A, $p>0.05$, n=6), and compared with that in normal control group, the survival rate of cardiomyocytes was notably decreased in high glucose group, showing a statistically significant difference ($p<0.05$). In addition, no difference was found in the survival rate of cardiomyocytes between high glucose + 1 μmol/L Epalrestat group and high glucose group, while it was substantially raised in high glucose + 10 μmol/L Epalrestat group compared with that in high glucose group, showing a statistically significant difference ($p<0.05$). Similarly, the LDH assay results revealed that there was no statistical difference in the cardiomyocyte toxicity between normal control group and mannitol group (Figure 3B, $p>0.05$, n=6), and compared with that in normal control group, the cardiomyocyte toxicity was notably increased in high glucose group, displaying a statistically significant difference ($p<0.05$). Additionally, cardiomyocyte toxicity was not different between high glucose + 1 μmol/L Epalrestat group and high glucose group, while it was substantially raised in high glucose +

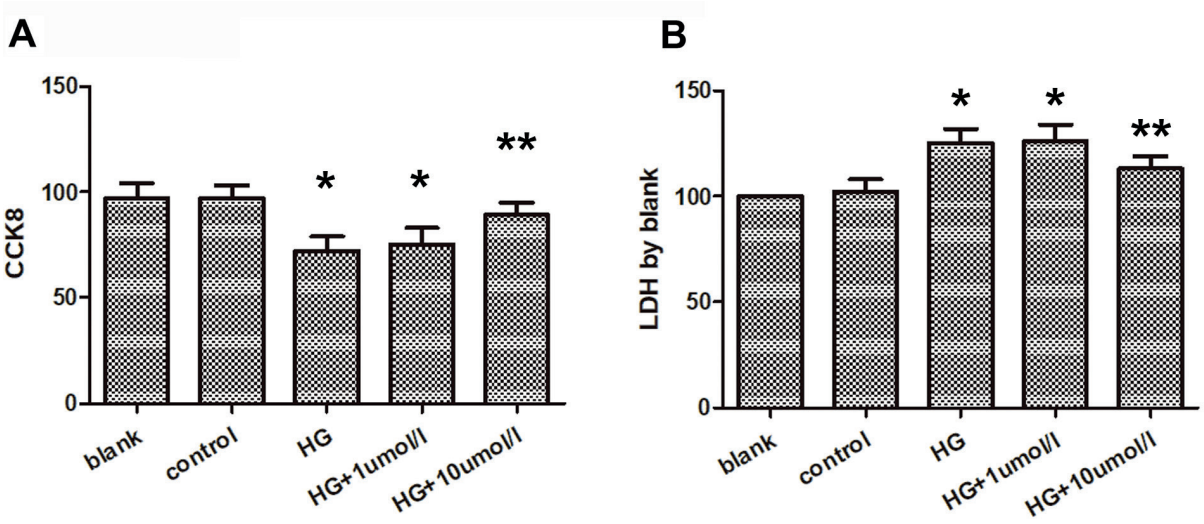

Figure 3. Epalrestat protects cultured cardiomyocytes from high glucose. ***A,*** CCK8 detects cell viability in blank, control, high glucose group, 1 umol/L epalrestat treatment group, and 10 umol/l epalrestat treatment group. ***B,*** LDH detects cytotoxicity in blank, control, high glucose group, 1 umol/L epalrestat treatment group, and 10 umol/L epalrestat treatment group.* Compared with the blank group, $p<0.05$, ** compared with the high sugar group, $p<0.05$

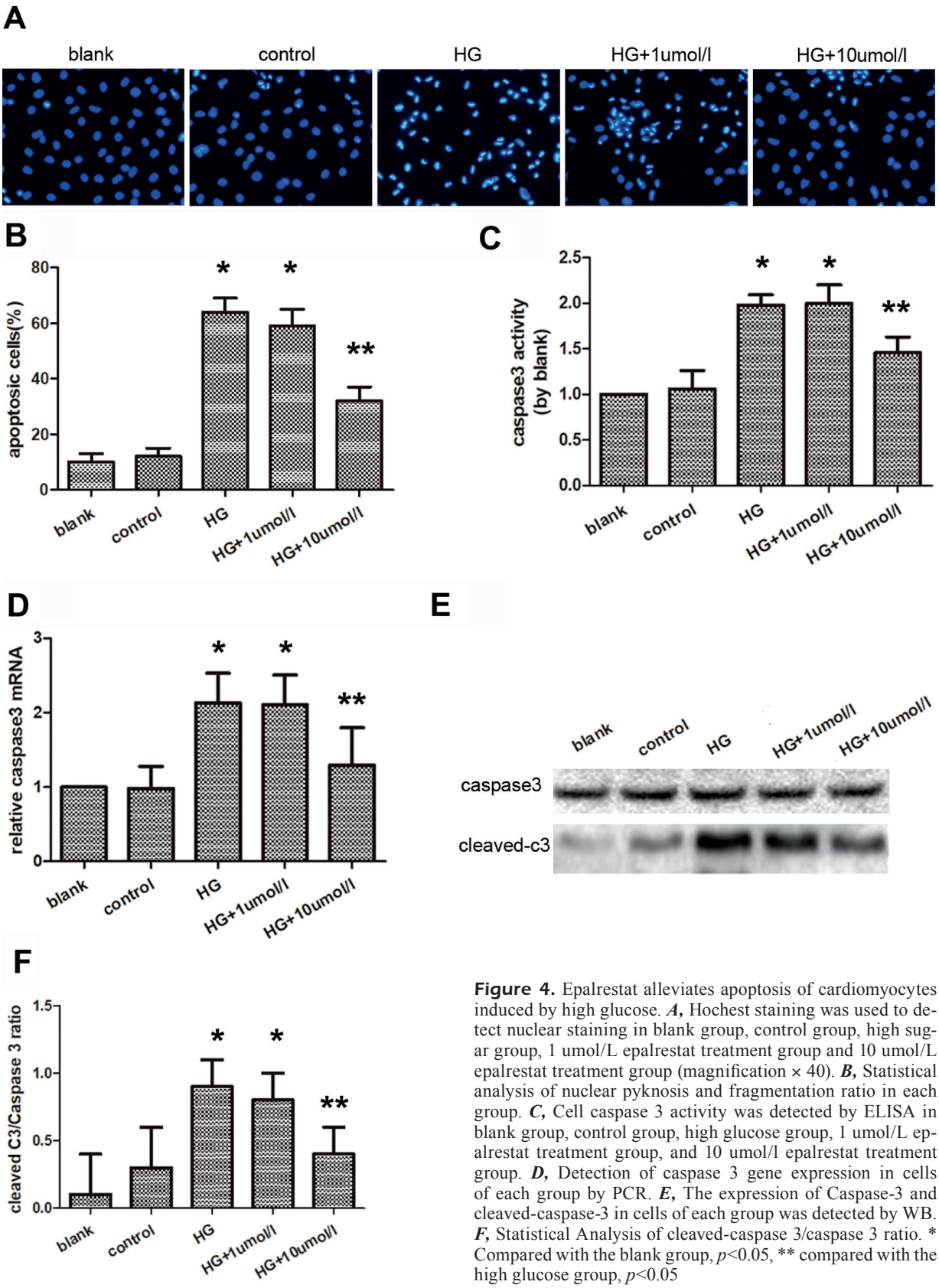

Figure 4. Epalrestat alleviates apoptosis of cardiomyocytes induced by high glucose. ***A,*** Hochest staining was used to detect nuclear staining in blank group, control group, high sugar group, 1 umol/L epalrestat treatment group and 10 umol/L epalrestat treatment group (magnification × 40). ***B,*** Statistical analysis of nuclear pyknosis and fragmentation ratio in each group. ***C,*** Cell caspase 3 activity was detected by ELISA in blank group, control group, high glucose group, 1 umol/L epalrestat treatment group, and 10 umol/l epalrestat treatment group. ***D,*** Detection of caspase 3 gene expression in cells of each group by PCR. ***E,*** The expression of Caspase-3 and cleaved-caspase-3 in cells of each group was detected by WB. ***F,*** Statistical Analysis of cleaved-caspase 3/caspase 3 ratio. * Compared with the blank group, $p<0.05$, ** compared with the high glucose group, $p<0.05$

10 μmol/L Epalrestat group compared with that in high glucose group, displaying a statistically significant difference ($p<0.05$).

Epalrestat Alleviated High Glucose-Induced Cardiomyocyte Apoptosis

Hoechst staining results revealed that compared with that in normal control group, the proportion of cells with karyopyknosis was evidently raised in high glucose group, displaying a statistically significant difference (Figure 4A, 4B, $p<0.05$, n=6). Moreover, it was not different between high glucose + 1 μmol/L Epalrestat group and high glucose group, but significantly decreased in high glucose + 10 μmol/L Epalrestat group compared with that in high glucose group. Also, $p<0.05$ was a statistically significant difference. PCR results indicated that high glucose group had a markedly higher gene expression level of Caspase-3 than normal control group, with a statistical difference (Figure 4C, $p<0.05$, n=6), and that it was evidently lowered in high glucose + 10 μmol/L Epalrestat group compared with that in high glucose group. Also, $p<0.05$ was a statistically significant difference. It was found through enzyme-linked immunosorbent assay (ELISA) that the activity of Caspase-3 in high glucose group was significantly higher than that in normal control group, with a statistical difference (Figure 4D, $p<0.05$, n=6), and that it was evidently lowered in high glucose + 10 μmol/L Epalrestat group compared with that in high glucose group, showing a statistically significant difference ($p<0.05$). According to the WB results, the proportion of cleaved-Caspase-3 was significantly raised in high glucose group compared with that in normal control group, showing a statistical difference (Figure 4E, 4F, $p<0.05$, n=6), while the proportion was evidently lowered in high glucose + 10 μmol/L Epalrestat group compared with that in high glucose group, displaying a statistically significant difference ($p<0.05$).

Epalrestat Inhibited the Oxidative Stress in Cardiomyocytes

The detection results revealed that inhibition of AR activity was markedly decreased in high glucose group compared with that in normal control group (Figure 5A, $p<0.05$, n=6), and that there was no difference between high glucose + 1 μmol/L Epalrestat group and high glucose group, while it was evidently increased in high glucose + 10 μmol/L Epalrestat group compared with that in high glucose group ($p<0.05$). The NO synthase (NOS) gene expression was detected *via* PCR. It was discovered that the expression level of NOS gene was markedly lowered in high glucose group compared with that in normal control group, showing a statistical difference (Figure 5B, $p<0.05$, n=6) and that it was evidently raised in high glucose + 10 μmol/L Epalrestat group compared with that in high glucose group ($p<0.05$). According to the determination results, the concentration of NO in high glucose group was significantly lower than that in normal control group (Figure 5C, $p<0.05$, n=6) and it was evidently higher in high glucose + 10 μmol/L Epalrestat group than that in high glucose group ($p<0.05$). Additionally, high glucose group had a markedly higher level of ROS produced in cardiomyocytes than normal control group (Figure 5D, $p<0.05$, n=6), while the production level of ROS in cardiomyocytes was substantially reduced in high glucose + 10 μmol/L Epalrestat group compared with that in high glucose group, showing a statistically significant difference (Figure 5E, $p<0.05$, n=6). The JC-1 staining results manifested that the mitochondrial membrane potential was significantly decreased in high glucose group compared with that in normal control group ($p<0.05$), and it was higher in high glucose + 10 μmol/L Epalrestat group than that in high glucose group ($p<0.05$).

Discussion

A major cause of multiple diabetes-related complications is the abnormality of the polyol pathway directly induced by high glucose[8]. In recent years, the key enzymes in the polyol pathway, namely, AR and ARIs, have attracted much attraction[9]. With Epalrestat, an ARI widely applied in clinic, as the research object, the present study found that it exerted a protective effect against high glucose-induced cardiomyocyte injuries. Namely, it inhibited AR activity to attenuate oxidative stress and mitochondrial injury in cardiomyocytes, and reduce high glucose-induced cardiomyocyte apoptosis. Excessive activation of AR can result in circulatory disorders, and affect the activity of vascular endothelial and myocardial cells[5], thus weakening their reactivity to bioactive substances such as histamine and platelet-activating factor, aortas' reactivity to phenylephrine, and the relaxation

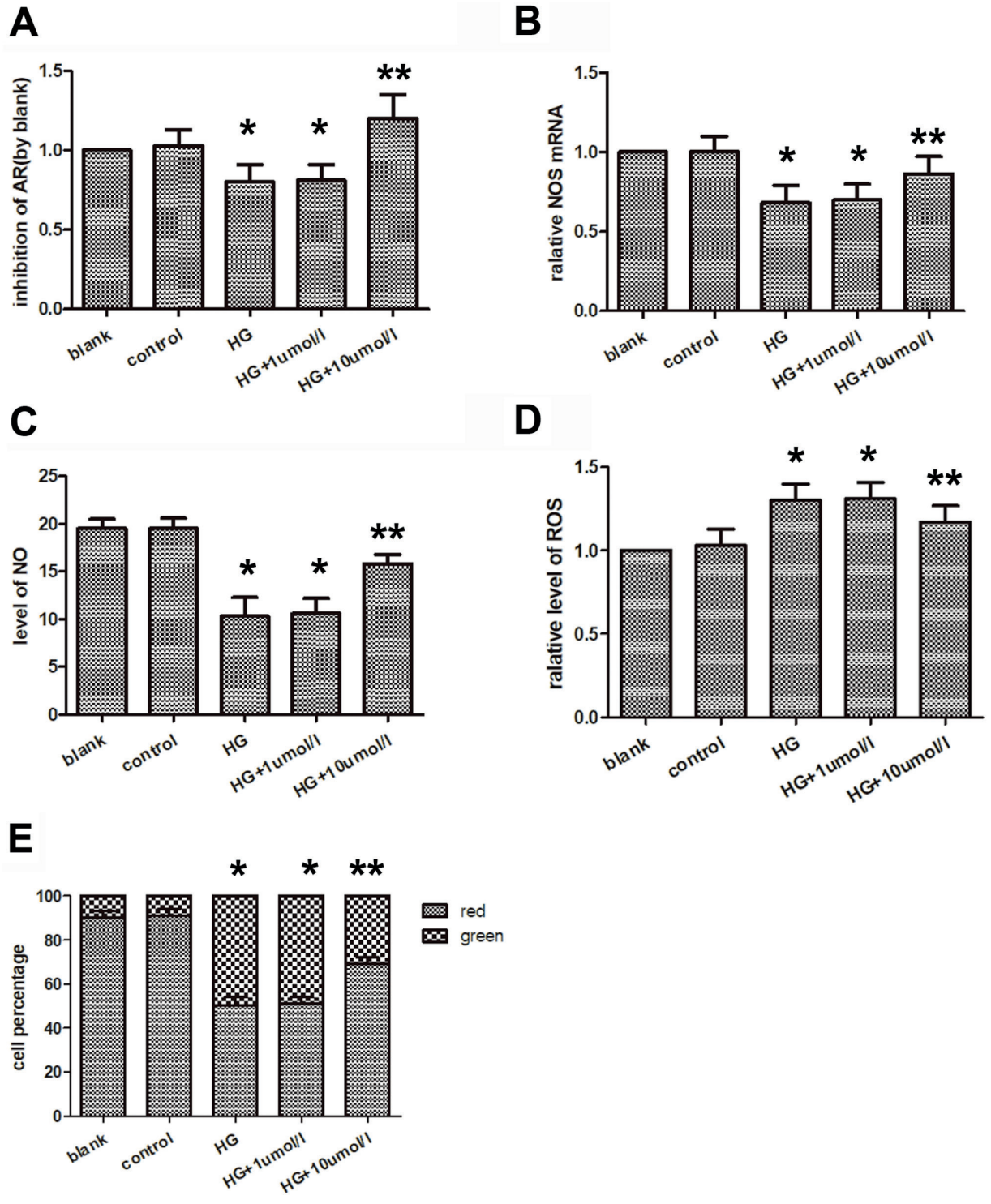

Figure 5. Epalrestat ameliorates oxidative stress induced by high glucose in cardiomyocytes. ***A,*** Detection of Cell AR inhibition was measured in blank group, control group, high sugar group, 1 umol/L epalrestat treatment group, and 10 umol/L epalrestat treatment group. ***B,*** Detection of NOS mRNA expression in cells of each group by PCR. ***C,*** Detection of NO Concentration in Cells of Different Groups. ***D,*** Detection of ROS concentration in cells of each group. ***E,*** Detection of mitochondrial membrane potential changes in each group by JC-1. * Compared with the blank group, $p<0.05$, ** compared with the high glucose group, $p<0.05$

of vascular endothelial cells by acetylcholine[4]. The intervention with ARIs can improve the microvascular reactivity to bradykinin, histamine, platelet-activating factor, and so on, significantly enhance the maximal contractile response of aortas to phenylephrine action, and restore acetylcholine-dependent vasodilation in endothelium[10,11]. The above effects may be realized through NOS.

It has been found in clinical research that Epalrestat, non-competitive ARIs, is capable of relieving diabetic peripheral neuropathy, autonomic neuropathy, fundus disease, and renal lesions[11-13]. Also, there were few findings in the study of diabetic cardiomyopathy: the diabetic patients with neuropathy and decreased cardiac ejection fraction were randomly divided into ARI treatment group and placebo group. The 1-year follow-up results showed that the left ventricular ejection fraction, cardiac output, and left ventricular stroke volume under resting conditions, as well as left ventricular ejection fraction in motion state, were notably improved in ARI treatment group. The efficacy was independent of blood pressure, insulin use, and abnormal heart rate variability under baseline conditions, while the cardiac output, stroke volume, and end-diastolic volume were all lowered in placebo group[14]. The above results indicate that ARIs repress and even partially reverse the worsening of diabetic cardiac function.

In this research, the high glucose-induced cardiomyocyte injury model was constructed, and it was discovered that Epalrestat alleviated high glucose-induced oxidative stress and inhibition on NO, reduced ROS production, and protected the mitochondrial membrane potential from changes under oxidative stress, ultimately weakening the activation of the intracellular apoptosis pathway, decreasing the proportion of apoptotic cells, and relieving high glucose-induced myocardial cytotoxicity. This explains why Epalrestat can improve the disease conditions in diabetic patients with cardiac insufficiency to some extent and provides a theoretical basis for the treatment in those with diabetic cardiomyopathy.

Conclusions

We found that Epalrestat inhibited AR activity to alleviate oxidative stress, thereby improving high glucose-induced cardiomyocyte injuries.

Conflict of Interests

The Authors declare that they have no conflict of interests.

References

1) Hong XY, Lin J, Gu WW. Risk factors and therapies in vascular diseases: an umbrella review of updated systematic reviews and meta-analyses. J Cell Physiol 2019; 234: 8221-8232.
2) Yuan T, Yang T, Chen H, Fu D, Hu Y, Wang J, Yuan Q, Yu H, Xu W, Xie X. New insights into oxidative stress and inflammation during diabetes mellitus-accelerated atherosclerosis. Redox Biol 2019; 20: 247-260.
3) Huynh K, Bernardo BC, McMullen JR, Ritchie RH. Diabetic cardiomyopathy: mechanisms and new treatment strategies targeting antioxidant signaling pathways. Pharmacol Ther 2014; 142: 375-415.
4) Volpe C, Villar-Delfino PH, Dos AP, Nogueira-Machado JA. Cellular death, reactive oxygen species (ROS) and diabetic complications. Cell Death Dis 2018; 9: 119.
5) Huang Z, Hong Q, Zhang X, Xiao W, Wang L, Cui S, Feng Z, Lv Y, Cai G, Chen X, Wu D. Aldose reductase mediates endothelial cell dysfunction induced by high uric acid concentrations. Cell Commun Signal 2017; 15: 3.
6) Paul M, Hemshekhar M, Kemparaju K, Girish KS. Berberine mitigates high glucose-potentiated platelet aggregation and apoptosis by modulating aldose reductase and NADPH oxidase activity. Free Radic Biol Med 2019; 130: 196-205.
7) Huang Q, Liu Q, Ouyang D. Sorbinil, an aldose reductase inhibitor, in fighting against diabetic complications. Med Chem 2019; 15: 3-7.
8) Jin QS, Huang LJ, Zhao TT, Yao XY, Lin LY, Teng YQ, Kim SH, Nam MS, Zhang LY, Jin YJ. HOXA11-AS regulates diabetic arteriosclerosis-related inflammation via PI3K/AKT pathway. Eur Rev Med Pharmacol Sci 2018; 22: 6912-6921.
9) Soltesova Prnova M, Svik K, Bezek S, Kovacikova L, Karasu C, Stefek M. 3-Mercapto-5H-1,2,4-triazino[5,6-b]indole-5-acetic acid (Cemtirestat) alleviatessymptoms of peripheral diabetic neuropathy in Zucker diabetic fatty (ZDF) rats: arole of aldose reductase. Neurochem Res 2019; 44: 1056-1064.
10) Alam F, Shafique Z, Amjad ST, Bin AM. Enzymes inhibitors from natural sources with antidiabetic activity: a review. Phytother Res 2019; 33: 41-54.
11) Senthilkumari S, Sharmila R, Chidambaranathan G, Vanniarajan A. Epalrestat, an aldose reductase inhibitor prevents glucose-induced toxicity in human retinal pigment epithelial cells in vitro. J Ocul Pharmacol Ther 2017; 33: 34-41.
12) He J, Gao HX, Yang N, Zhu XD, Sun RB, Xie Y, Zeng CH, Zhang JW, Wang JK, Ding F, Aa JY, Wang GJ. The aldose reductase inhibitor epalrestat exerts nephritic protection on diabetic nephropathy in db/db mice through metabolic modulation. Acta Pharmacol Sin 2019; 40: 86-97.

13) Hotta N, Kawamori R, Fukuda M, Shigeta Y; Aldose Reductase Inhibitor-Diabetes Complications Trial Study Group. Long-term clinical effects of epalrestat, an aldose reductase inhibitor, on progression of diabetic neuropathy and other microvascular complications: multivariate epidemiological analysis based on patient background factors and severity of diabetic neuropathy. Diabet Med 2012; 29: 1529-1533.
14) Hu X, Li S, Yang G, Liu H, Boden G, Li L. Efficacy and safety of aldose reductase inhibitor for the treatment of diabetic cardiovascular autonomic neuropathy: systematic review and meta-analysis. PLoS One 2014; 9: e87096.